



Cite this: *Energy Environ. Sci.*, 2021, 14, 5523

## Solvent-controlled O<sub>2</sub> diffusion enables air-tolerant solar hydrogen generation†

Michael G. Allan,<sup>a</sup> Morgan J. McKee,<sup>a</sup> Frank Marken<sup>b</sup> and Moritz F. Kuehnel   <sup>ac</sup>

Solar water splitting into H<sub>2</sub> and O<sub>2</sub> is a promising approach to provide renewable fuels. However, the presence of O<sub>2</sub> hampers H<sub>2</sub> generation and most photocatalysts show a major drop in activity in air without synthetic modification. Here, we demonstrate efficient H<sub>2</sub> evolution in air, simply enabled by controlling O<sub>2</sub> diffusion in the solvent. We show that in deep eutectic solvents (DESs), photocatalysts retain up to 97% of their H<sub>2</sub> evolution activity and quantum efficiency under aerobic conditions whereas in water, the same catalysts are almost entirely quenched. Solvent-induced O<sub>2</sub> tolerance is achieved by H<sub>2</sub> generation outcompeting O<sub>2</sub>-induced quenching due to low O<sub>2</sub> diffusivities in DESs combined with low O<sub>2</sub> solubilities. Using this mechanism, we derive design rules and demonstrate that applying these rules to H<sub>2</sub> generation in water can enhance O<sub>2</sub> tolerance to >34%. The simplicity and generality of this approach paves the way for enhancing water splitting without adding complexity.

Received 14th June 2021,  
Accepted 20th August 2021

DOI: 10.1039/d1ee01822a

rsc.li/ees

### Broader context

Green hydrogen production is a key process for the transition to a carbon-neutral economy, but oxygen, ubiquitous in air and generated during water splitting, interferes with hydrogen generation. Not only does the presence of O<sub>2</sub> lower the hydrogen evolution efficiency, it can also degrade hydrogen evolution catalysts; in addition, O<sub>2</sub> causes problems in other key energy technologies, such as Li–O<sub>2</sub> batteries, fuel cells and in many other redox processes. The current approaches to improving O<sub>2</sub> tolerance add complexity and often come at the expense of consuming redox equivalents for O<sub>2</sub> removal, which lowers the overall efficiency. Here we show that by simply choosing solvents with a low O<sub>2</sub> diffusivity and solubility, photocatalysts normally inefficient for H<sub>2</sub> generation in air become highly O<sub>2</sub> tolerant, with minimal loss in activity and efficiency in air, even for extended periods of time. By unravelling the mechanism of the solvent-induced O<sub>2</sub> tolerance, we can translate it to achieve oxygen tolerance even in water, making it an important new concept with general applicability independent of the catalyst, solvent or process – a key step in making green H<sub>2</sub> production simpler and more efficient on a global scale.

## Introduction

Solar hydrogen production from water is viewed as a viable method for generating clean renewable fuel to aid in combatting global energy challenges.<sup>1,2</sup> Materials employed for solar-driven H<sub>2</sub> production should be considered based on their cost, stability, toxicity and most importantly their practical applicability on a large scale. Real-world photocatalytic H<sub>2</sub> production systems must be active in the presence of O<sub>2</sub> generated *in situ* by water splitting and by exposure to air.<sup>3</sup> However, H<sub>2</sub> evolution in an aerobic environment is usually suppressed because of the more favourable oxygen reduction reaction.<sup>4</sup> In addition,

molecular O<sub>2</sub> can inhibit H<sub>2</sub> evolution co-catalysts *via* interaction with the active site or by forming reactive oxygen species (ROSS).<sup>5,6</sup> Proton reduction in the presence of O<sub>2</sub> has been achieved by developing electrocatalysts with selectivity for H<sub>2</sub> evolution over O<sub>2</sub> reduction<sup>7</sup> or by creating a local anaerobic environment around the catalyst. Methods of lowering the effective O<sub>2</sub> concentration at the catalyst include O<sub>2</sub> reduction at catalysts capable of performing both O<sub>2</sub> reduction and H<sup>+</sup> evolution<sup>8–10</sup> and at organic dyes,<sup>11</sup> constructing layered architectures in which O<sub>2</sub> is reduced before it reaches the active site,<sup>12–14</sup> introducing antioxidant additives,<sup>15,16</sup> and modifying catalytic sites with O<sub>2</sub>-blocking layers.<sup>17–19</sup> However, these approaches require a costly re-design of the catalyst to enhance O<sub>2</sub> tolerance and in many cases photons and charges are used to reduce O<sub>2</sub>, leading to a decrease in quantum and faradaic yield, respectively. Recent work has demonstrated O<sub>2</sub>-tolerant CO<sub>2</sub> reduction enabled by controlling O<sub>2</sub> diffusion to the electrode using selective membranes and coatings.<sup>20,21</sup> Related approaches have been used in lithium–oxygen batteries.<sup>22</sup>

<sup>a</sup> Department of Chemistry, Swansea University, Singleton Park, Swansea SA2 8PP, Wales, UK. E-mail: m.f.kuehnel@swansea.ac.uk

<sup>b</sup> Department of Chemistry, University of Bath, Claverton Down, Bath BA2 7AY, UK

<sup>c</sup> Fraunhofer Institute for Microstructure of Materials and Systems IMWS, Walter-Hülse-Straße 1, 06120 Halle, Germany

† Electronic supplementary information (ESI) available: Experimental details, additional tables and figures. See DOI: 10.1039/d1ee01822a



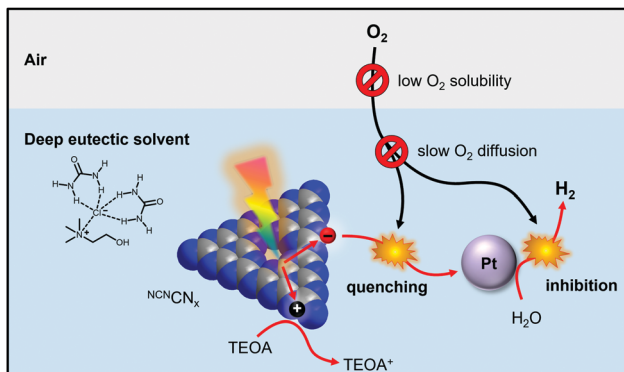


Fig. 1 Schematic representation of solvent-mediated oxygen-tolerant photocatalytic hydrogen production in deep eutectic solvents demonstrated in this work.

To date, research in hydrogen evolution has not exploited solvent effects for promoting  $O_2$  tolerance, even though  $O_2$  solubility and diffusivity in the reaction medium are the primary factors controlling the availability of  $O_2$  to the catalytically active site.

In this work we demonstrate that using deep eutectic solvents (DESs) as a reaction medium enables  $O_2$ -tolerant photocatalytic  $H_2$  production with  $O_2$ -intolerant photocatalysts without making any catalyst modifications and without affecting the quantum efficiency. DESs are an alternative class of low-cost, highly tuneable ionic liquids<sup>23</sup> that can be prepared from readily available precursors and possess lower toxicities than conventional ionic liquids.<sup>24</sup> DESs have been employed for air-tolerant organic reactions involving highly reactive organolithium compounds<sup>25,26</sup> and it has recently been shown they can stabilise  $O_2$ -sensitive radicals in air.<sup>27</sup> Using a carbon nitride photocatalyst, we now show that DESs create a near-anaerobic environment in which up to 97% of the photocatalytic  $H_2$  evolution activity is retained under air (Fig. 1). Mechanistic studies reveal a close interplay between  $O_2$  solubility and diffusivity and allow us to develop a quantitative model of the  $O_2$  tolerance. Based on this model we derive key design criteria for tailored reaction media that promote efficient and cost-effective  $O_2$  tolerance with established  $H_2$  generation photocatalysts without synthetic modification.

## Results and discussion

### Deep eutectic solvents as a medium for solar $H_2$ generation

To investigate solvent effects on the photocatalytic  $H_2$  evolution performance, we chose cyanamide-functionalised carbon nitride ( $^{NCN}CN_x$ ) as a model photocatalyst (Fig. S1–S4, ESI<sup>†</sup>)<sup>28,29</sup> and studied its activity in three well-known type-III DESs, namely choline chloride–urea 1:2, choline chloride–glycerol 1:2, and choline chloride–ethylene glycol 1:2, termed reline, glycine and ethaline, respectively. These solvents were chosen due to their facile preparation, low cost, low toxicity and infinite miscibility with water.<sup>23</sup> Pt was used as a HER co-catalyst, *in situ* photodeposited from  $H_2PtCl_6$  ( $Pt^{NCN}CN_x$ ). In reline,  $Pt^{NCN}CN_x$  generated  $138.3 \pm 2.6 \mu\text{mol}_{H_2}$  after 14 h

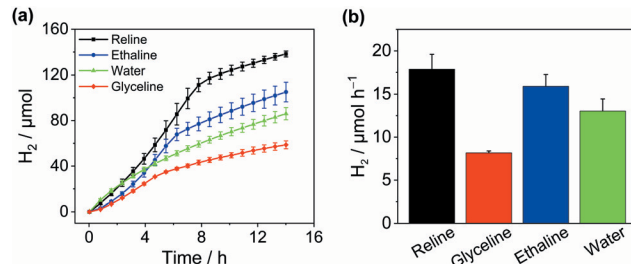


Fig. 2 Photocatalytic  $H_2$  generation in DESs at  $Pt/^{NCN}CN_x$ : (a)  $H_2$  production in different DESs and water; (b) max.  $H_2$  production rate in DESs vs.  $H_2O$ . Conditions:  $^{NCN}CN_x$  (2.0 mg),  $H_2PtCl_6$  (0.05 mg Pt), in 2.0 mL DES (12.5% v/v  $H_2O$ , 0.38 M TEOA, 2 mM  $MV^{2+}$ ) or water (0.38 M TEOA, pH 7, no  $MV^{2+}$ ); AM 1.5G, 1 sun, 40 °C, constant  $N_2$  purge.

irradiation with simulated solar light (AM 1.5G, 1 sun) at an activity of  $8.9 \pm 0.9 \text{ mmol}_{H_2} \text{ g}_{CN_x}^{-1} \text{ h}^{-1}$  using triethanolamine (TEOA) as a sacrificial electron donor (Fig. 2). Addition of water (12.5% by volume) was essential as in neat DESs,  $H_2$  evolution activity was negligible (Fig. S5, ESI<sup>†</sup>). The same conditions yielded an activity of  $8.0 \pm 0.6$  and  $4.1 \pm 0.1 \text{ mmol}_{H_2} \text{ g}_{CN_x}^{-1} \text{ h}^{-1}$  for ethaline and glycine, respectively with cumulative values of  $105.1 \pm 8.6$  and  $58.7 \pm 3.5 \mu\text{mol}_{H_2}$  after 14 hours (Table S1, ESI<sup>†</sup>). Depending on the solvent, a decay in activity was observed after 5–9 h which we attribute to the well-known decomposition of the redox mediator methyl viologen ( $MV^{2+}$ )<sup>30</sup> as with a further addition of  $MV^{2+}$ , the rate increased again (Fig. S6, ESI<sup>†</sup>). In the absence of  $MV^{2+}$ ,  $H_2$  evolution was slower but no decay in activity was observed (Fig. S7, ESI<sup>†</sup>) proving that the DESs do not compromise the stability of the  $^{NCN}CN_x$  photocatalyst. In water,  $^{NCN}CN_x$  displayed a maximum activity of  $6.5 \pm 0.7 \text{ mmol}_{H_2} \text{ g}_{CN_x}^{-1} \text{ h}^{-1}$  and a cumulative production of  $86.1 \pm 5.4 \mu\text{mol}_{H_2}$  after 14 h irradiation under optimised conditions (0.38 M TEOA, pH 7.0, no  $MV^{2+}$ ) which is on par with recent literature values.<sup>29</sup> This was lower in comparison to reline and ethaline and higher than the activity in glycine (see Fig. S8 and S9, ESI<sup>†</sup> for optimisation and controls). The external quantum efficiency for  $H_2$  evolution in reline was determined at  $3.7 \pm 1.5\%$  and was stable even after 20 h of irradiation (Table S2, ESI<sup>†</sup>). We can therefore state that under the given conditions, DESs are a competitive solvent with water for solar  $H_2$  generation.

A notable difference between water and DES is the effect of added  $MV^{2+}$  on the  $H_2$  evolution: While adding  $MV^{2+}$  increases  $H_2$  generation in DES, a decrease in activity is observed in water (Fig. S10, ESI<sup>†</sup>). A suppression of  $H_2$  evolution upon addition of the redox mediator  $MV^{2+}$  has been previously observed in cases where there is good electron transfer between the photocatalyst and the HER co-catalyst.<sup>31</sup> In this case, adding  $MV^{2+}$  does not enhance HER but instead causes a visible accumulation of reduced  $MV^{+}$  in the solution which blocks light penetration to the photocatalyst due to its deep blue colour. The beneficial effects of adding  $MV^{2+}$  in DESs, in turn, suggest poor electron transfer between  $^{NCN}CN_x$  and Pt in DESs. To prove this, we performed recycling experiments in which we separated the photocatalyst after 4 h irradiation in the presence of  $H_2PtCl_6$



from its supernatant and re-suspended it in a fresh solution without added Pt, before continuing irradiation. In water, the photocatalytic  $H_2$  evolution activity was not affected by this procedure, suggesting Pt is deposited on the  $^{NCN}CN_x$  photocatalyst (Fig S11, ESI<sup>†</sup>), in line with previous literature. In DES, however, the photocatalytic activity was almost completely quenched, corroborating poor immobilisation of Pt on  $^{NCN}CN_x$  in DES, possibly due to differences in solvation in DESs.

### O<sub>2</sub>-tolerant H<sub>2</sub> generation in DESs

Inspired by their application as solvents to perform air-sensitive syntheses under an aerobic atmosphere,<sup>25,26</sup> we set out to achieve air-tolerant  $H_2$  evolution in DESs. It is well known that photocatalytic  $H_2$  evolution is suppressed in air even for highly active materials<sup>32</sup> arising from the thermodynamically favourable O<sub>2</sub> reduction and quenching of the photosensitiser. Fig. 3a indicates that Pt/ $^{NCN}CN_x$  generates only  $0.8 \pm 0.2 \text{ mmol}_{H_2} \text{ g}_{CN_x}^{-1} \text{ h}^{-1}$  upon irradiation in aerated water corresponding to a retention of only  $8.8 \pm 1.5\%$  of its photocatalytic activity seen under inert conditions. When the redox mediator MV<sup>2+</sup> was added the retention dropped to  $1.7 \pm 0.7\%$ . However, in the DES reline, the same catalyst without any modification achieved an activity of up to  $8.7 \pm 0.9 \text{ mmol}_{H_2} \text{ g}_{CN_x}^{-1} \text{ h}^{-1}$  in air, corresponding to a remarkable activity retention of up to  $97.3 \pm 17.5\%$  compared to anaerobic conditions (Fig. 3b and Table S3, ESI<sup>†</sup>). While the O<sub>2</sub> tolerance in water decreases further over time with almost complete deactivation after 10 h, DESs maintain a high level of O<sub>2</sub> tolerance over prolonged periods of time (Fig. S12, ESI<sup>†</sup>). After 14 h,  $123.5 \pm 8.1 \mu\text{mol}_{H_2}$  were produced

in air (Fig. 3c) corresponding to  $89.3 \pm 6.1\%$  of the amount produced under N<sub>2</sub> and the system remained active (Fig. 3d). Similarly, an activity of  $5.7 \pm 1.3 \text{ mmol}_{H_2} \text{ g}_{CN_x}^{-1} \text{ h}^{-1}$  was seen in aerobic ethaline ( $73.5 \pm 9.0\%$  retention) and  $3.6 \pm 0.3 \text{ mmol}_{H_2} \text{ g}_{CN_x}^{-1} \text{ h}^{-1}$  in aerobic glycine ( $90.4 \pm 7.9\%$  retention). The external quantum efficiency for  $H_2$  evolution in aerobic reline was determined at  $3.9 \pm 0.3\%$  after 20 h of irradiation (Table S4, ESI<sup>†</sup>) which is within error identical to the EQE observed in anaerobic conditions. The optimum O<sub>2</sub> tolerance was observed at 12.5% water content. Increasing the water content led to a lower O<sub>2</sub> tolerance (Fig. S13, ESI<sup>†</sup>), whereas without added water,  $H_2$  evolution activity was much lower, presumably for lack of available protons (Fig. S5, ESI<sup>†</sup>).

The O<sub>2</sub> tolerance induced by DESs compares favourably with examples of O<sub>2</sub>-tolerant  $H_2$  evolution from the literature (Table S5, ESI<sup>†</sup>). A range of CdS-based photocatalysts<sup>33–35</sup> achieve O<sub>2</sub> tolerances between 40–80%; air can even increase the activity of CdS by suppressing photocorrosion.<sup>36</sup> These studies typically operate at high  $H_2$  production rates due to high electron donor concentrations, closed photoreactors and often high light intensities, where O<sub>2</sub> in the solution and the reactor headspace is rapidly depleted by reduction to H<sub>2</sub>O, effectively generating anaerobic conditions *in situ*. This is often indicated by an observed lag period before  $H_2$  evolution occurs. In contrast,  $H_2$  production in DESs shows no detectable lag period and a high O<sub>2</sub> tolerance despite a continuous air purge maintaining a constant O<sub>2</sub> concentration. The latter is particularly important to exploit O<sub>2</sub> tolerance to enhance overall water splitting, where O<sub>2</sub> is continuously generated and  $H_2$  production rates are much lower than in sacrificial systems. Photocatalysts operating at lower rates where O<sub>2</sub> depletion is less effective have shown lower O<sub>2</sub> tolerances, *e.g.* RuP/CoP/TiO<sub>2</sub> (17% O<sub>2</sub> tolerance),<sup>9</sup> Ni<sub>2</sub>P/OH-GQD (64%)<sup>37</sup> and PFBT polymer dots (37%).<sup>38</sup> To the best of our knowledge, there is no literature on O<sub>2</sub>-tolerant  $H_2$  generation using carbon nitride-based photocatalysts.

The advantage of solvent-induced O<sub>2</sub> tolerance lies in its applicability independent of the photocatalyst. When Pt/TiO<sub>2</sub> was used as the photocatalyst instead of Pt/ $^{NCN}CN_x$ , the O<sub>2</sub> tolerance similarly increased from  $29.6 \pm 6.5\%$  in water to  $86.1 \pm 12.8\%$  in reline after 12 h irradiation (Fig. S14, ESI<sup>†</sup>), proving this effect is not limited to a single photocatalyst. To further demonstrate the generality of this approach, we also studied  $H_2$  evolution at the homogeneous photocatalyst Pt/Eosin Y (Pt/EY).<sup>39</sup> Even though the  $H_2$  evolution in ethaline and reline ( $17.5 \pm 1.7 \mu\text{mol}_{H_2} \text{ mmol}_{EY}^{-1}$  and  $11.4 \pm 1.7 \mu\text{mol}_{H_2} \text{ mol}_{EY}^{-1}$  after 5.5 h, respectively, non-optimised conditions, Fig. S15, ESI<sup>†</sup>) was slower than in water ( $81.1 \pm 6.8 \mu\text{mol}_{H_2} \text{ mmol}_{EY}^{-1}$ ), the DESs promote excellent retention of activity in air. Pt/EY in aerobic H<sub>2</sub>O produced  $0.7 \text{ mmol}_{H_2} \text{ mol}_{EY}^{-1}$  after 5.5 h (<1% activity retained), whereas  $14.9 \mu\text{mol}_{H_2} \text{ mol}_{EY}^{-1}$  was generated in ethaline corresponding to 85.5% O<sub>2</sub> tolerance. This, again, compares well with literature examples of aerobic  $H_2$  evolution at homogeneous photocatalysts,<sup>40–42</sup> *e.g.* CoP/EY retained  $70 \pm 4\%$  activity in air, however activity was limited to 2 h.<sup>9</sup>

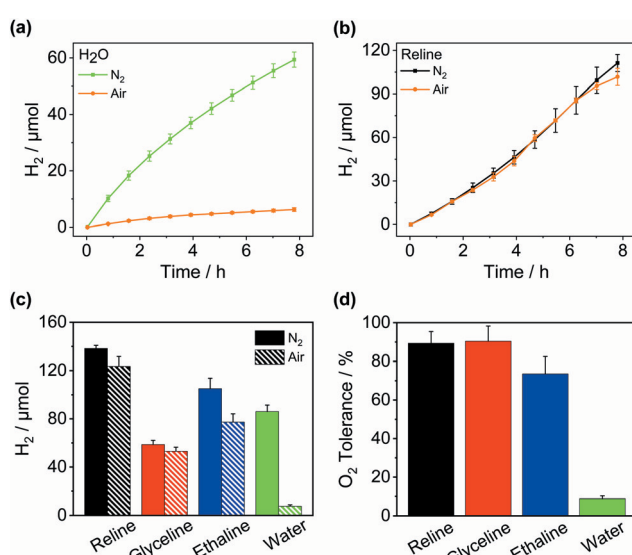


Fig. 3 Solvent-mediated oxygen-tolerant  $H_2$  generation at Pt/ $^{NCN}CN_x$ . Effect of aerobic conditions on  $H_2$  production in (a) H<sub>2</sub>O and (b) reline; (c) total  $H_2$  evolved after 14.0 h under anaerobic and aerobic conditions in different DESs and H<sub>2</sub>O; (d) relative  $H_2$  evolution activities under aerobic conditions depending on the solvent. Conditions:  $^{NCN}CN_x$  (2.0 mg) H<sub>2</sub>PtCl<sub>6</sub> (0.05 mg Pt) in 2.0 mL DES (12.5% v/v H<sub>2</sub>O, 0.38 M TEOA, 2 mM MV<sup>2+</sup>) or water (0.38 M TEOA, pH 7); AM 1.5G, 1 sun, 40 °C, constant air purge.



## The mechanism of solvent-induced O<sub>2</sub> tolerance

Having demonstrated that DESs promote O<sub>2</sub> tolerance of photocatalytic H<sub>2</sub> evolution independent of the photocatalyst, we sought to gain understanding of the underlying mechanism. Previous work on DESs enabling air-tolerant alkylation with organolithium and Grignard reagents suggested that the high halide concentration in DESs increases the reagents' reactivity to levels where they can outcompete hydrolysis. However, no explanation for the observed insensitivity to O<sub>2</sub> was given.<sup>25,43</sup> To elucidate the mechanism by which DESs promote O<sub>2</sub>-tolerant H<sub>2</sub> evolution, we first studied the formation and stability of reduced <sup>N</sup>CN<sub>x</sub><sup>\*</sup> in both H<sub>2</sub>O and DESs in air. <sup>N</sup>CN<sub>x</sub> is known to form a turquoise-blue photoreduced state <sup>N</sup>CN<sub>x</sub><sup>\*</sup> originating from charge accumulation in the material when irradiated in the presence of an electron donor and absence of a hydrogen evolution co-catalyst.<sup>29</sup> <sup>N</sup>CN<sub>x</sub><sup>\*</sup> persists in an anaerobic environment but is quenched rapidly by reaction with O<sub>2</sub>. In water, <sup>N</sup>CN<sub>x</sub><sup>\*</sup> is therefore only formed under N<sub>2</sub> and immediately quenched upon exposure to air as indicated by the blue material regaining its original yellow colour. However, when <sup>N</sup>CN<sub>x</sub> is irradiated in DESs, <sup>N</sup>CN<sub>x</sub><sup>\*</sup> is quickly formed even in an aerated solution. Moreover, the blue colour is stable in air for several days, with a noticeable absorbance at  $\sim$ 680 nm in the DR-UV spectrum, ascribed to the reduced photocatalyst (Fig. 4). This absorbance is not observed in an aerated aqueous solution, highlighting the solvent effect on limiting the quenching of the photoabsorber by reaction with O<sub>2</sub>. To further corroborate the absence of O<sub>2</sub> quenching in aerated DESs, we investigated photocatalytic degradation of the organic dye methylene blue in aerated DESs using <sup>N</sup>CN<sub>x</sub> as a photocatalyst. Dye degradation relies on reactive oxygen species (ROSs) such as O<sub>2</sub><sup>·</sup> to act as oxidants, generated by the quenching of the excited state of a photocatalyst by O<sub>2</sub>; it is therefore strongly dependant on dissolved O<sub>2</sub>.<sup>44</sup> Consistently, we observed that the degradation of methylene blue was much slower in DESs than in water, which lends further evidence to a suppression of O<sub>2</sub> quenching depending on the solvent (Fig. S16, ESI†).

Further quantitative insight was sought from determining the saturation concentration and diffusion coefficient of O<sub>2</sub> in DESs by studying the electrochemical O<sub>2</sub> reduction at a Pt

**Table 1** O<sub>2</sub> solubility and diffusivity in different solvents determined by microwire chronoamperometry and observed O<sub>2</sub> tolerance during photocatalytic H<sub>2</sub> generation in these solvents. Conditions: DES (12.5% H<sub>2</sub>O, 0.38 M TEOA, 2 mM MV) or water (0.38 M TEOA, pH 7), 40 °C; photocatalysis: <sup>N</sup>CN<sub>x</sub> (2.0 mg), H<sub>2</sub>PtCl<sub>6</sub> (0.05 mg Pt) in 2.0 mL solvent, (AM 1.5G, 1 sun, constant air purge)

Solvent	c(O <sub>2</sub> ) [μM]	D(O <sub>2</sub> ) [m <sup>2</sup> s <sup>-1</sup> ]	O <sub>2</sub> tolerance <sup>a</sup> [%]
Reline	167.8 $\pm$ 9.1	2.93 $\pm$ 0.02 $\times$ 10 <sup>-10</sup>	89.3 $\pm$ 6.1
Ethaline	250.7 $\pm$ 0.4	3.32 $\pm$ 0.01 $\times$ 10 <sup>-10</sup>	73.5 $\pm$ 9.0
Glyceline	218.8 $\pm$ 2.0	9.52 $\pm$ 0.01 $\times$ 10 <sup>-11</sup>	90.4 $\pm$ 7.9
H <sub>2</sub> O	223.5 $\pm$ 0.4	2.94 $\pm$ 0.01 $\times$ 10 <sup>-9</sup>	8.8 $\pm$ 1.5 <sup>b</sup>

<sup>a</sup> O<sub>2</sub> tolerance = total H<sub>2</sub> produced under air relative to total H<sub>2</sub> produced under N<sub>2</sub> at Pt/<sup>N</sup>CN<sub>x</sub> after 14 h irradiation under otherwise identical conditions. <sup>b</sup> Without added MV<sup>2+</sup>.

microwire electrode.<sup>45</sup> Potential step chronoamperometry was performed in each solvent and the observed current transients for the electrocatalytic O<sub>2</sub> reduction were fitted according to the Shoup-Szabo equation<sup>46</sup> to simultaneously derive the O<sub>2</sub> concentrations and the O<sub>2</sub> diffusion coefficients in aerated DESs and water, under the conditions tested for photocatalytic H<sub>2</sub> evolution (Table 1 and Fig. S17–S20, ESI†).<sup>47</sup> All the DES-based solutions exhibited lower O<sub>2</sub> solubilities than conventional organic solvents,<sup>48,49</sup> presumably due to their high ionic strengths causing a salting-out effect.<sup>50,51</sup> In addition, O<sub>2</sub> diffusion coefficients were found to be lower than in most other solvents<sup>48,49</sup> including water<sup>52</sup> but varied strongly between the different DESs. This behaviour is likely a result of their high viscosities combined with their complex liquid structure,<sup>53</sup> in which hydrogen bond donor dependent cluster formation presumably influences molecular diffusion in the liquid as well as causing large variations in viscosity.<sup>54</sup>

We expect O<sub>2</sub> tolerance to be a function of the effective O<sub>2</sub> concentration at the photocatalyst surface, which depends on both solubility and diffusivity of O<sub>2</sub> in the reaction medium. Comparing the trends in these parameters for the different DES-based solutions to the trend in O<sub>2</sub> tolerance shows a clear correlation between the observed retention of photocatalytic activity in air (glyceline  $\approx$  reline  $>$  ethaline  $>$  water) and the O<sub>2</sub> diffusivities (glyceline  $<$  reline  $<$  ethaline  $<$  water). As O<sub>2</sub> in solution is being consumed due to O<sub>2</sub> reduction at the photocatalyst, the steady-state O<sub>2</sub> concentration at the catalyst surface depends on how rapidly more O<sub>2</sub> is supplied to the photocatalyst, therefore O<sub>2</sub> tolerance is primarily dominated by the O<sub>2</sub> diffusivity. The O<sub>2</sub> solubility of the solutions (reline  $<$  glyceline  $<$  ethaline  $<$  water) is of secondary importance: glyceline and reline solutions show comparable O<sub>2</sub> tolerances despite them showing varying O<sub>2</sub> solubilities and diffusivities – this is likely because the lower diffusivity in glyceline is compensated by a higher O<sub>2</sub> solubility, and *vice versa*. Water shows poor O<sub>2</sub> tolerance because it exhibits the highest O<sub>2</sub> diffusion coefficient among the solvents studied here and a relatively high O<sub>2</sub> solubility. Due to a combination of low O<sub>2</sub> diffusivities and low O<sub>2</sub> solubilities, DESs thus create pseudo-inert conditions by limiting O<sub>2</sub> mass transport, which is outcompeted by H<sup>+</sup> diffusion.

Having identified the combination of low O<sub>2</sub> solubility and O<sub>2</sub> diffusivity as key factors to O<sub>2</sub> tolerance, we use these design

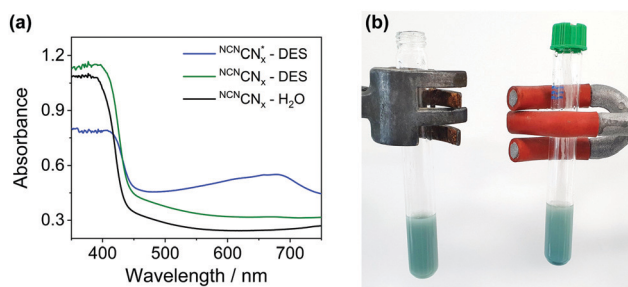


**Fig. 4** (a) Absorption spectra of <sup>N</sup>CN<sub>x</sub> in DES TEOA solution (green trace) and aqueous TEOA solution (black trace) prior to irradiation with simulated solar light. <sup>N</sup>CN<sub>x</sub><sup>\*</sup> absorption spectra in DES TEOA solution (blue) recorded in ambient air. (b) Photo of <sup>N</sup>CN<sub>x</sub><sup>\*</sup> in DES solutions exposed to air (left) and in inert atmosphere (right).



**Table 2**  $O_2$  solubility and diffusivity in brines of different concentration and observed  $O_2$  tolerance during photocatalytic  $H_2$  generation. Conditions:  $^{NCN}CN_x$  (2.0 mg),  $H_2PtCl_6$  (0.05 mg Pt) in 2.0 mL water (0.38 M TEOA, pH 7, 2 mM  $MV^{2+}$ ); (AM 1.5G, 1 sun, 40 °C, constant air purge)

Solvent <sup>a</sup>	$c(O_2)$ [μM]	$D(O_2)$ [m <sup>2</sup> s <sup>-1</sup> ]	$O_2$ tolerance <sup>b</sup> [%]
0 M NaCl	223 ± 0.4	$2.94 \pm 0.01 \times 10^{-9}$	3.1 ± 1.7
1 M NaCl	265 ± 0.6	$2.30 \pm 0.01 \times 10^{-9}$	13.9 ± 3.3
2 M NaCl	165 ± 0.2	$1.55 \pm 0.01 \times 10^{-9}$	19.0 ± 11.4
4 M NaCl	128 ± 0.3	$1.13 \pm 0.01 \times 10^{-9}$	34.2 ± 4.4

<sup>a</sup> Solubilities were determined under the same conditions as the photocatalysis experiments were performed. <sup>b</sup>  $O_2$  tolerance = total  $H_2$  produced under air relative to total  $H_2$  produced under  $N_2$  at  $Pt/^{NCN}CN_x$  after 14 h irradiation under otherwise identical conditions.

criteria to promote  $O_2$  tolerance in other solvents. Saline water is an attractive feedstock for renewable  $H_2$  production since seawater is much more abundant than freshwater and its use avoids competition with drinking water supplies.<sup>55</sup> While using seawater can be challenging, we show here that it can enable highly  $O_2$ -tolerant  $H_2$  evolution. It is well known that high salt concentrations lower the  $O_2$  solubility in water as well as the  $O_2$  diffusion coefficients.<sup>47,56</sup> We therefore determined the  $O_2$  solubility and diffusivity in brines under photocatalysis conditions (40 °C, 0.38 M TEOA, pH 7) by microwire electrochemistry. Table 2 shows that the  $O_2$  solubility and diffusivity both decrease by approx. 50% upon increasing the NaCl concentration from 0 to 4 M. Consistently, Fig. 5 demonstrates that in line with our identified design criteria, the  $O_2$  tolerance in water increases with increasing NaCl concentrations. In 4 M aqueous NaCl a cumulative  $O_2$  tolerance of  $34.2 \pm 4.4\%$  is observed after 14 h (Fig. S21 and Table S6, ESI†), more than 10 times higher than without added NaCl (Table 2). However,

despite lower  $O_2$  solubilities, the  $O_2$  tolerance never reaches the levels observed in DESs consistent with the higher  $O_2$  diffusion coefficient in water. This demonstrates that the  $O_2$  diffusivity is decisive for the overall  $O_2$  tolerance, ideally when paired with a low  $O_2$  solubility. Furthermore, we studied the direct use of seawater collected from Swansea Beach as a solvent for  $H_2$  evolution (Fig. S22, ESI†). While the  $H_2$  generation activity was lower than in pure brines, presumably due to its brownish colour, the observed  $O_2$  tolerance of  $7.2 \pm 4.4\%$  was higher than in pure DI water. Considering the local salinity of 0.41–0.53 M,<sup>57</sup> this data is in good agreement with Table 2 and demonstrates the usefulness of using non-potable water for solar  $H_2$  generation.

### Design rules from a quantitative model for $O_2$ tolerance

To explain the effect of  $O_2$  diffusivity and solubility on the  $O_2$  tolerance quantitatively, we have developed a mechanistic model based on fluxes to and from the photocatalyst particles (Fig. 6a). The rate of charge carrier generation,  $R(h\nu)$ , depends on light intensity and quantum efficiency and is assumed largely independent of the solvent.  $O_2$  is expected to quench charge carriers with consuming  $O_2$ , expressed as the rate  $R(O_2)$ . Approximating the  $O_2$ -dependent quenching as  $O_2$  reduction at a spherical particle at the limit of diffusional control gives eqn (1):

$$R(O_2) = 4\pi \times r \times n \times D(O_2) \times c(O_2) \quad (1)$$

with  $r$  the particle radius and  $n$  the number of electrons quenched per  $O_2$  molecule.<sup>47</sup> The flux of  $H_2$  from the particle,  $R(H_2)$ , is assumed not impeded. The  $O_2$  tolerance can then be expressed as the efficiency of  $H_2$  production in competition with  $O_2$ -dependent quenching (eqn (2)), which upon expressing  $R(O_2)$  according to eqn (1) shows a linear dependence of the  $O_2$  tolerance on the product of  $D(O_2)$  and  $c(O_2)$  (eqn (3)):

$$O_2 \text{ tolerance} = 100\% \times \frac{R(H_2)}{R(h\nu)} = 100\% \times \frac{R(h\nu) - R(O_2)}{R(h\nu)} \quad (2)$$

$$O_2 \text{ tolerance} = \left( 1 - \frac{4\pi rn}{R(h\nu)} \times D(O_2) \times c(O_2) \right) \quad (3)$$

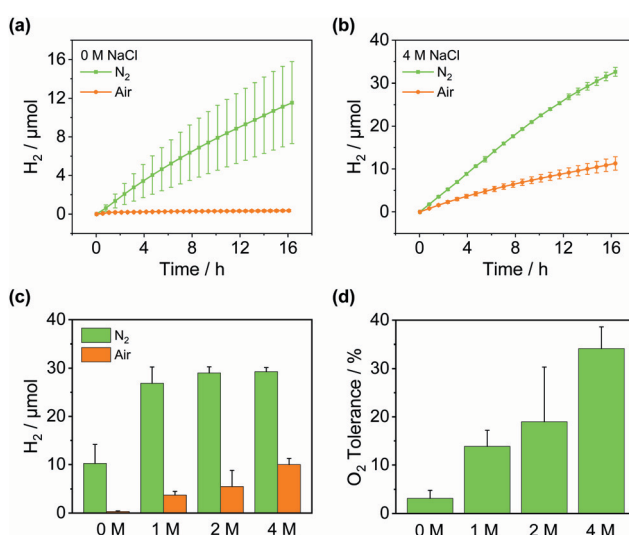


**Fig. 5** Enhanced oxygen tolerance by control of  $O_2$  diffusion. Effect of aerobic conditions on  $H_2$  production in (a)  $H_2O$  and (b) 4 M aqueous NaCl; (c) total  $H_2$  evolved after 14.0 h depending on the NaCl concentration and atmosphere; (d)  $O_2$  tolerance of  $H_2$  evolution depending on the NaCl concentration. Conditions:  $^{NCN}CN_x$  (2.0 mg),  $H_2PtCl_6$  (0.05 mg Pt) in 2.0 mL saline water (0.38 M TEOA, pH 7, 2 mM  $MV^{2+}$ ); AM 1.5G, 1 sun, 40 °C, constant  $N_2$  or air purge.

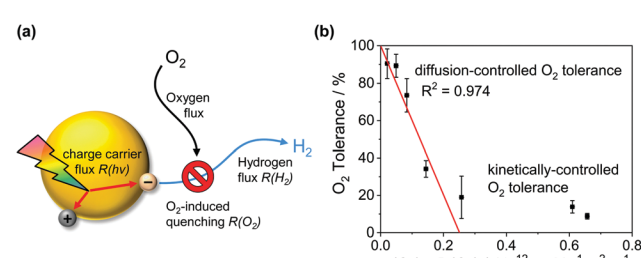


**Fig. 6** Mechanistic model for the solvent-induced  $O_2$  tolerance. (a) Schematic illustration of fluxes to and from the photocatalyst particle. (b) Plot of the  $O_2$  tolerance for  $H_2$  evolution versus the product of  $D(O_2)$  and  $c(O_2)$  in the respective reaction medium fitted according to eqn (3).

Fig. 6 shows that the experimentally observed  $O_2$  tolerances fit well to this model (see ESI† for details). At high  $O_2$  tolerances, the slope represents the consumption of photo-generated charge carriers by  $O_2$  in diffusion-limited quenching. When the  $O_2$  flux increases with higher  $O_2$  solubility and diffusivity, the quenching process is no longer diffusion limited but instead kinetically limited by the rate of  $O_2$  reduction, resulting in  $O_2$  tolerance gradually tailing towards zero at a much lower slope. From this model, we can infer a set of design rules for improving  $O_2$  tolerance through further solvent design:

1. Minimise the  $c \times D$  parameter (low  $O_2$  solubility and diffusivity, high viscosity).
2. Decrease particle size (large particles increase  $O_2$  flux).
3. Increase light intensity (outcompete  $O_2$  flux which is independent of light).
4. Increase photon-to-charge carrier conversion.

Future work should focus on exploring all variables of the model to further verify and refine its predictive ability and achieve sustained, fully  $O_2$ -tolerant  $H_2$  generation.

## Conclusions

We have shown that  $O_2$ -tolerant  $H_2$  evolution can be achieved by controlling  $O_2$  diffusion and solubility in the reaction medium. We introduced DESs as a versatile medium for solar  $H_2$  generation with both heterogenous and homogenous light absorbers and showed that DESs induce a high  $O_2$  tolerance to otherwise  $O_2$ -intolerant photocatalysts without compromising the quantum efficiency. We demonstrated this effect results from their low  $O_2$  solubilities and diffusivities. Exploiting these properties as design criteria enables a 10-fold increase in  $O_2$  tolerance in water by controlling  $O_2$  diffusion and solubility. Through developing a quantitative model for oxygen tolerance, we believe this investigation paves the way for further solvent-enhanced solar fuel production and, owing to the tuneable nature of DESs, allows for a wide scope of solvents to be examined. The fact that a relatively small change in the solvent constituents (replacing ethylene glycol with glycerol) causes a considerable change in the  $O_2$  diffusivity and thus in the  $O_2$  tolerance demonstrates the enormous potential of solvent design for solar water splitting, yet it highlights the need for establishing structure–function relationships to allow a rational solvent design. Future studies will expand the concept of  $O_2$  diffusion control to fully explore all parameters of our model with the potential to massively enhance solar water splitting without adding complexity.

## Data availability

Raw experimental data is openly available via dx.doi.org/10.5281/zenodo.5236823.

## Author contributions

MFK conceived, supervised and led the project. MGA conducted most of the experimental work and analysed the data.

MJM performed dye degradation experiments. FM conceived and supervised electrochemical measurements. MFK, MGA and FM wrote the manuscript.

## Conflicts of interest

The authors declare no conflict of interest.

## Acknowledgements

This work was supported by EPSRC through a DTA studentship to MGA (EP/R51312X/1), and a capital investment grant to MFK (EP/S017925/1). We thank Swansea University for providing start-up funds to MFK. We thank Prof. Alex Cowan and Dr Gaia Neri (University of Liverpool) for recording DR-UV spectra. We wish to thank Julian Kivell and Phil Hopkins in the Swansea University mechanical workshop for their assistance with the experimental setup. MFK is grateful to the Ernst Schering Foundation for support.

## References

- 1 Y. Tachibana, L. Vayssières and J. Durrant, *Nat. Photonics*, 2012, **6**, 511–518.
- 2 Q. Wang and K. Domen, *Chem. Rev.*, 2020, **120**, 919–985.
- 3 D. W. Wakerley and E. Reisner, *Energy Environ. Sci.*, 2015, **8**, 2283–2295.
- 4 P. M. Wood, *Biochem. J.*, 1988, **253**, 287–289.
- 5 M. T. Stiebitz and M. Reiher, *Chem. Sci.*, 2012, **3**, 1739–1751.
- 6 B. Mondal and A. Dey, *Chem. Commun.*, 2017, **53**, 7707–7715.
- 7 S. Chatterjee, K. Sengupta, S. Dey and A. Dey, *Inorg. Chem.*, 2013, **52**, 14168–14177.
- 8 N. Kaeffer, A. Morozan and V. Artero, *J. Phys. Chem. B*, 2015, **119**, 13707–13713.
- 9 F. Lakadamyalı, M. Kato, N. M. Muresan and E. Reisner, *Angew. Chem., Int. Ed.*, 2012, **51**, 9381–9384.
- 10 Z.-H. Pan, Y.-W. Tao, Q.-F. He, Q.-Y. Wu, L.-P. Cheng, Z.-H. Wei, J.-H. Wu, J.-Q. Lin, D. Sun, Q.-C. Zhang, D. Tian and G.-G. Luo, *Chem. – Eur. J.*, 2018, **24**, 8275–8280.
- 11 T. Sakai, D. Mersch and E. Reisner, *Angew. Chem., Int. Ed.*, 2013, **52**, 12313–12316.
- 12 H. Li, D. Buesen, S. Dementin, C. Léger, V. Fourmond and N. Plumeré, *J. Am. Chem. Soc.*, 2019, **141**, 16734–16742.
- 13 A. Ruff, J. Szczesny, N. Marković, F. Conzuelo, S. Zacarias, I. A. C. Pereira, W. Lubitz and W. Schuhmann, *Nat. Commun.*, 2018, **9**, 3675.
- 14 C. Tapia, R. D. Milton, G. Pankratova, S. D. Minteer, H.-E. Åkerlund, D. Leech, A. L. De Lacey, M. Pita and L. Gorton, *ChemElectroChem*, 2017, **4**, 90–95.
- 15 S. Dey, A. Rana, D. Crouthers, B. Mondal, P. K. Das, M. Y. Darensbourg and A. Dey, *J. Am. Chem. Soc.*, 2014, **136**, 8847–8850.



16 Z. Li, B. Tian, W. Zhen, Y. Wu and G. Lu, *Appl. Catal., B*, 2017, **203**, 408–415.

17 K. Maeda, K. Teramura, D. Lu, N. Saito, Y. Inoue and K. Domen, *Angew. Chem., Int. Ed.*, 2006, **45**, 7806–7809.

18 A. T. Garcia-Esparza, T. Shinagawa, S. Ould-Chikh, M. Qureshi, X. Peng, N. Wei, D. H. Anjum, A. Clo, T.-C. Weng, D. Nordlund, D. Sokaras, J. Kubota, K. Domen and K. Takanabe, *Angew. Chem., Int. Ed.*, 2017, **56**, 5780–5784.

19 W. J. Jo, G. Katsoukis and H. Frei, *Adv. Funct. Mater.*, 2020, **30**, 1909262.

20 H. Li, U. Münchberg, A. A. Oughli, D. Buesen, W. Lubitz, E. Freier and N. Plumeré, *Nat. Commun.*, 2020, **11**, 920.

21 Y. Xu, J. P. Edwards, J. Zhong, C. P. O'Brien, C. M. Gabardo, C. McCallum, J. Li, C.-T. Dinh, E. H. Sargent and D. Sinton, *Energy Environ. Sci.*, 2020, **13**, 554–561.

22 X.-D. Lin, Y. Gu, X.-R. Shen, W.-W. Wang, Y.-H. Hong, Q.-H. Wu, Z.-Y. Zhou, D.-Y. Wu, J.-K. Chang, M.-S. Zheng, B.-W. Mao and Q.-F. Dong, *Energy Environ. Sci.*, 2021, **14**, 1439–1448.

23 E. L. Smith, A. P. Abbott and K. S. Ryder, *Chem. Rev.*, 2014, **114**, 11060–11082.

24 A. K. Halder and M. N. D. S. Cordeiro, *ACS Sustainable Chem. Eng.*, 2019, **7**, 10649–10660.

25 C. Vidal, J. García-Álvarez, A. Hernán-Gómez, A. R. Kennedy and E. Hevia, *Angew. Chem., Int. Ed.*, 2014, **53**, 5969–5973.

26 D. Arnodo, S. Ghinato, S. Nejrotti, M. Blangetti and C. Prandi, *Chem. Commun.*, 2020, **56**, 2391–2394.

27 J. A. McCune, M. F. Kuehnel, E. Reisner and O. A. Scherman, *Chem.*, 2020, **6**, 1819–1830.

28 V. W.-H. Lau, I. Moudrakovski, T. Botari, S. Weinberger, M. B. Mesch, V. Duppel, J. Senker, V. Blum and B. V. Lotsch, *Nat. Commun.*, 2016, **7**, 12165.

29 W. Yang, R. Godin, H. Kasap, B. Moss, Y. Dong, S. A. J. Hillman, L. Steier, E. Reisner and J. R. Durrant, *J. Am. Chem. Soc.*, 2019, **141**, 11219–11229.

30 M. Heyrovský, *J. Chem. Soc., Chem. Commun.*, 1987, 1856–1857.

31 E. Reisner, D. J. Powell, C. Cavazza, J. C. Fontecilla-Camps and F. A. Armstrong, *J. Am. Chem. Soc.*, 2009, **131**, 18457–18466.

32 L. Ma, M. Liu, D. Jing and L. Guo, *J. Mater. Chem. A*, 2015, **3**, 5701–5707.

33 Z. Sun, H. Zheng, J. Li and P. Du, *Energy Environ. Sci.*, 2015, **8**, 2668–2676.

34 D. A. Reddy, H. Park, S. Hong, D. P. Kumar and T. K. Kim, *J. Mater. Chem. A*, 2017, **5**, 6981–6991.

35 S. Cao, Y. Chen, C.-J. Wang, X.-J. Lv and W.-F. Fu, *Chem. Commun.*, 2015, **51**, 8708–8711.

36 D. W. Wakerley, K. H. Ly, N. Kornienko, K. L. Orchard, M. F. Kuehnel and E. Reisner, *Chem. – Eur. J.*, 2018, **24**, 18385–18388.

37 L. Zhu, Q. Yue, D. Jiang, H. Chen, R. M. Irfan and P. Du, *Chin. J. Catal.*, 2018, **39**, 1753–1761.

38 L. Wang, R. Fernández-Terán, L. Zhang, D. L. A. Fernandes, L. Tian, H. Chen and H. Tian, *Angew. Chem., Int. Ed.*, 2016, **55**, 12306–12310.

39 L. Wang, H. Zhao, Y. Chen, R. Sun and B. Han, *Opt. Commun.*, 2016, **370**, 122–126.

40 T. R. Canterbury, S. M. Arachchige, K. J. Brewer and R. B. Moore, *Chem. Commun.*, 2016, **52**, 8663–8666.

41 L. Petermann, R. Staehle, M. Pfeifer, C. Reichardt, D. Sorsche, M. Wächtler, J. Popp, B. Dietzek and S. Rau, *Chem. – Eur. J.*, 2016, **22**, 8240–8253.

42 A. Call, Z. Codolà, F. Acuña-Parés and J. Lloret-Fillol, *Chem. – Eur. J.*, 2014, **20**, 6171–6183.

43 C. Vidal, J. García-Álvarez, A. Hernán-Gómez, A. R. Kennedy and E. Hevia, *Angew. Chem., Int. Ed.*, 2016, **55**, 16145–16148.

44 J. Schneider, D. Bahnemann, J. Ye, G. L. Puma and D. D. Dionysiou, *Photocatalysis: Fundamentals and Perspectives*, Royal Society of Chemistry, Cambridge, 2016.

45 A. Neudeck and L. Kress, *J. Electroanal. Chem.*, 1997, **437**, 141–156.

46 A. Szabo, D. K. Cope, D. E. Tallman, P. M. Kovach and R. M. Wightman, *J. Electroanal. Chem. Interfacial Electrochem.*, 1987, **217**, 417–423.

47 J. Weber, A. J. Wain and F. Marken, *Electroanalysis*, 2015, **27**, 1829–1835.

48 J. D. Wadhawan, P. J. Welford, H. B. McPeak, C. E. W. Hahn and R. G. Compton, *Sens. Actuators, B*, 2003, **88**, 40–52.

49 A. Schürmann, R. Haas, M. Murat, N. Kuritz, M. Balaish, Y. Ein-Eli, J. Janek, A. Natan and D. Schröder, *J. Electrochem. Soc.*, 2018, **165**, A3095–A3099.

50 K. Onda, E. Sada, T. Kobayashi, S. Kito and K. Ito, *J. Chem. Eng. Jpn.*, 1970, **3**, 18–24.

51 W. Lang and R. Zander, *Ind. Eng. Chem. Fundam.*, 1986, **25**, 775–782.

52 W. Xing, M. Yin, Q. Lv, Y. Hu, C. Liu and J. Zhang, in *Rotating Electrode Methods and Oxygen Reduction Electrocatalysts*, ed. W. Xing, G. Yin and J. Zhang, Elsevier, Amsterdam, 2014, pp. 1–31.

53 O. S. Hammond, D. T. Bowron and K. J. Edler, *Angew. Chem., Int. Ed.*, 2017, **56**, 9782–9785.

54 A. Y. M. Al-Murshedi, H. F. Alesary and R. Al-Hadrawi, *J. Phys.: Conf. Ser.*, 2019, **1294**, 052041.

55 W. Tong, M. Forster, F. Dionigi, S. Dresp, R. Sadeghi Erami, P. Strasser, A. J. Cowan and P. Farràs, *Nat. Energy*, 2020, **5**, 367–377.

56 S. L. Clegg and P. Brimblecombe, *Geochim. Cosmochim. Acta*, 1990, **54**, 3315–3328.

57 J. A. M. Abbas, PhD thesis, Swansea University, 1986.

